ELSEVIER

International Journal of Heat and Fluid Flow 20 (1999) 552–561

International Journal of HEAT AND FLUID FLOW

www.elsevier.com/locate/ijhff

A finite conductivity model for diesel spray evaporation computations

C. Bertoli, M.na Migliaccio *

Istituto Motori-C.N.R. D.I.M.E. Università degli Studi di Napoli 'Federico II', Naples, Italy

Abstract

The authors present some spray calculations in a combustion bomb and in a d.i. diesel engine for different test cases varying the formulation of the evaporation model in a modified version of the 3D-fluidynamic KIVA II code. Some numerical tests cases have been performed in a combustion bomb to analyze the influence of the modified evaporation model on droplet heating, evaporation rate and droplet lifetime. The numerical results have been compared with those obtained from the original Spalding model and with some experimental data obtained by an optical technique. In a second set of calculations, the new model has been tested in the combustion chamber of a real d.i. diesel engine. Results in terms of pressure, vapour mass, spray distribution and burned fuel are reported. A preliminary analysis on exhaust emissions has been done.

1. Introduction

In diesel engines fuel evaporation plays an important role in determining air/fuel mixing. As a matter of fact, fuel vapor concentration and distribution in the combustion chamber directly influence the combustion evolution, and as a consequence, the exhaust emissions. In the past years, a great number of computational studies led to a better description of liquid fuel sprays during the evaporation process. Lately, the injection system has a more and more important role in improving spray characteristics and high pressure injection systems (Arcoumanis et al., 1997; Patterson et al., 1998; Tennison et al., 1998) are in common use; this can justify the greater attention to modelling, in a more efficient way, spray processes (such as the atomization and evaporation phenomena).

Evaporation of droplets involves simultaneous heat and mass transfer processes; heat for evaporation is transferred to the droplet surface by conduction, convection and radiation from the surrounding hot gases, while fuel vapour is transferred by convection and diffusion back into the gas stream.

In order to simulate a really complex phenomenon like diesel fuel spray evaporation a lot of assumptions have been commonly used. A classic droplet vaporisation model is the Spalding model (Spalding, 1953) as originally introduced in the KIVA II code. This model is based on many over-simplified assumptions: Gas boundary layer is quasi-steady; spherical symmetry is employed; radiation is neglected and air and fuel vapour behave as ideal gases; droplet temperature is spatially uniform; Fick's law of diffusion is assumed; vapour/liquid phase equilibrium occurs at the fuel surface; the "1/3 rule" is used for gas properties.

New evaporation models have been formulated to remove some over-simplified assumptions in the original Spalding model allowing to a better understanding of the evaporation under high pressure conditions (Shwing-Chung Wong and Ar-Cheng Lin, 1992) (as the diesel engine conditions at the injection time). Since convective unsteady effects have been found not to affect the heat transfer to the droplet, existing models usually assume quasi-steady conditions for the gaseous phase around the droplet. On the contrary, the adequate description of liquid phase, specially for multicomponent fuels, needs the modelling of the heat transferred by conduction within the droplet, internal droplet circulation, solubility and high pressure effects (Kneer et al., 1996; Varnavas and Assanis, 1996; Hohmann et al., 1996). In typical combustion situations, the duration of the transient droplet heating is comparable with the droplet vaporisation time; therefore, an adequate description of the internal heat transfer is needed. The transient heating is influenced by internal liquid circulation, which may only slightly change the time-scale of the internal heating process, Sirignano, (1978). Some other evaporation models have introduced the high-pressure effects on phase equilibrium, transport properties and surface tension and they have described the non-uniform temperature field inside the droplet, Arcoumanis et al., (1997).

The present work aims to further improve the description of liquid fuel sprays during the evaporation process in the combustion chamber of a direct injection diesel engine. As a matter of fact one of the most important hypotheses of the Spalding model assumes that the conduction heat transfer inside the droplet can be neglected. Using this assumption, the fuel thermal conductivity is assumed to be "infinite" and the temperature inside the droplet is uniformally equal to its surface temperature value. In order to introduce a more realistic transient heating of the droplet, more realistic values for fuel thermal conductivity have been introduced; thus the new evaporation model allows the calculation of the internal temperature distribution of the drop.

A large number of tests have been done simulating the conditions in a combustion bomb without considering break-up, collisions and coalescence phenomena. In a second set of calculation, the proposed model has been applied to the combustion chamber of a real d.i. diesel engine with different

* Corresponding author. E-mail: marianna@motori.im.na.cnr.it

0142-727X/99/$ – see front matter
PII: S0142-727X(99)00044-2

fuels, where the superposition of breakup, collisions and coalescence effects is evident. The analysis has been performed until the start of combustion for a diesel fuel by varying the breakup model. In this way the influence of the new evaporation model seems to join with the superposition of different break-up effects and droplet size distribution. Some results are reported in terms of spray characteristics, such as fuel tip penetration, Sauter mean diameter and vapour mass quantities. The vapour mass distribution in the combustion chamber is also evident in some graphs, where the iso-lines of fuel/air ratio are shown. Further numerical computations have been referred to the tetradecane fuel in order to analyze the influence of the proposed model on combustion evolution and some in-cylinder species emissions.

2. The proposed evaporation model

Numerical computations have been performed with a version of the Kiva-II code (Amsden et al., 1989) including some modifications with respect to the original version of the program.

First a spray-wall interaction model was added in the form described by Naber et al., (1988) and Amato et al. (1991). Some improvements were also introduced concerning the atomization process introducing a 'hybrid' model (Beatrice et al., 1995), based on the TAB (O'Rourke and Amsden, 1987) and the WAVE models (Reitz.,1987). The standard k–ε turbulence model was used adopting only a new value of the C_3 compressibility constant (−0.33). The ignition model (Belardini et al., 1996a,b) is developed based on the Nishida and Hiroyasu (1989) formula modified with the correlation of Hardenberg and Hase (1979). The NO formation is modelled with Zeldovich' mechanism in the form described by Bowman (1975). Finally the soot formation and oxidation mechanism is coupled with the combustion model by a reduced seven-step mechanism (Belardini et al., 1996a,b) characterised by the full coupling with the combustion mechanism.

The model characteristics are the following: the liquid fuel is injected; the fuel vaporisation and dispersion are computed as provided by the model described in the following. Simultaneously the fuel vapour turns to acetylene by a single step reaction

$$r1: \qquad C_nH_m \Rightarrow \frac{n}{2}C_2H_2 + \frac{m}{2}H_2.$$

The reaction rate is

$$\omega_1 = A_1 e^{-E_1/T}[C_nH_m].$$

Here and in the following terms in squared brackets are molar concentration in moles/cm^3; κ and ε are the turbulent kinetic energy and its dissipation rate; s is the stoichiometric ratio. A_i and E_i, whose values are reported later together with the other constants, are, respectively the pre-exponential factor and the activation temperature for the premixed combustion; B_2, B_3 are the proportional factors for the diffusive combustion. The acetylene formed is oxidised at high temperature by a single step stoichiometric reaction

$$r2: \qquad C_2H_2 + \frac{5}{2}O_2 \Longleftrightarrow 2CO_2 + H_2O.$$

The corresponding reaction rate has been expressed as

$$\omega_2 = \min(\omega_{\mathrm{premix}_2}, \omega_{\mathrm{diff}_2}),$$

where

$$\omega_{\mathrm{premix}_2} = A_2 e^{-E_2/T}[C_2H_2]^a[O_2]^b,$$

$$\omega_{\mathrm{diff}_2} = B_2 \frac{\varepsilon}{\kappa} * \min\left([C_2H_2], \frac{[O_2]}{s}\right).$$

Also the injected fuel is oxidised by

$$r3: \qquad C_nH_m + \left(n + \frac{m}{4}\right)O_2 \Longleftrightarrow nCO_2 + \frac{m}{2}H_2O$$

with the rate

$$\omega_3 = \min(\omega_{\mathrm{premix}_3}, \omega_{\mathrm{diff}_3})$$

also expressed as

$$\omega_{\mathrm{premix}_3} = A_3 e^{-E_3/T}[C_nH_m]^c[O_2]^d,$$

$$\omega_{\mathrm{diff}_3} = B_3 \frac{\varepsilon}{\kappa} * \min\left([C_nH_m], \frac{[O_2]}{s}\right).$$

The influence of heat diffusion within the liquid droplet has also been investigated (Golini, 1993) on single droplet vaporisation comparing the computational results with Hiroyasu's experimental data (Hiroyasu et al., 1980). The liquid phase description normally assumes uniform temperature distribution within the droplet. However, for diesel sprays with a very high internal cylinder pressure, this assumption is no longer valid because the resistance for heat and mass transfer in the gas film at the droplet surface are of the same order of magnitude as the resistances within the droplets (Aggarwal, 1987; Jin and Borman, 1985; Abramzon and Sirignano, 1988).

The proposed evaporation model allows for the droplets to be heated up as soon as they are injected in the combustion chamber of a diesel engine and a temperature distribution is immediately evident inside droplets. Under high ambient temperatures the influence of the heat conduction model on this dynamic process is significant; as a matter of fact, unlike the Spalding original evaporation model higher temperature values and higher thermal gradients appear on the drop external surface while the inner core of the droplet is still cool. The droplet surface heating and thus evaporation are faster mainly in the first part of the droplet lifetime. After the heat conduction flux reaches the droplet's center, droplet internal thermal gradients will decrease and a uniform temperature distribution will appear inside the droplet.

In the original Spalding evaporation model the droplet surface conditions are calculated from mass and energy balance:

$$\frac{d}{dt}\left(\frac{4}{3}\pi r^3 \rho_l\right) = -\dot{m}, \tag{1}$$

$$4\pi r^2 h_\infty (T_\infty - T) = m c_l \dot{T} + \dot{m} L, \tag{2}$$

where r is the droplet radius, T the droplet temperature, c_l and ρ_l are specific heat and density of the liquid, L the latent heat of vaporisation, T_∞ the ambient temperature, h_∞ the convection coefficient and $\dot{m}$ the mass transfer rate. From the energy balance (2) at the droplet surface, the convective heat flux from the surrounding gas is calculated by summing the heat transferred to the liquid phase and the latent heat of vaporisation calculated at the droplet surface temperature. In the proposed evaporation model the energy balance at droplet surface has been modified and accounts for the thermal conduction phenomenon inside the droplet. In order to describe the internal temperature distribution the Fourier equation in spherical coordinates for a 1D system must be solved in the proposed model

$$\frac{\partial T}{\partial t} = \frac{k_l}{\rho_l c_l}\frac{1}{r^2}\frac{\partial}{\partial r}\left(r^2 \frac{\partial T}{\partial r}\right). \tag{3}$$

The boundary conditions in the center and at the drop's surface are

$$(r=0)\quad \frac{\partial T}{\partial r}=0;\quad (r=r_s)\quad 4\pi r_s^2 h_\infty (T_\infty - T_s) = \dot{m}L + 4\pi r_s^2 k_l \left(\frac{\partial T}{\partial r}\right)_s, \tag{4}$$

where k_l is the fuel conductivity. The fuel thermal conductivity coefficient depends on fuel temperature as in Maxwell (1977). Some other fuel properties, like liquid internal energy and specific heat, are also variable with temperature and their values have been referred to the droplet mass mean temperature.

Following implicit solution for the finite-difference approximation of Eq. (3), the value of the droplet surface temperature is determined at every time step. In order to solve Eqs. (1) and (3) and determine the temperature distribution $T(r, t)$ an explicit solution has been used, and a maximum value for the time step Δt, not leading to numerical instabilities and using the minimum Δr, has been calculated as

$$\Delta t_{\text{num}} = \frac{(\Delta r)^2 \rho_l c_l}{2k_l}. \tag{5}$$

The time step in the evaporation process will be the minimum between this Δt_{num} and Δt_{ev} taken from the original evaporation model. The value of Δt_{ev} is obtained by the hypothesis that the heat transferred to the droplet cannot exceed a certain percentage of the cell energy (Amsden et al., 1989).

According to the hypothesis of a droplet spherical symmetry, droplets have been stratified with an initial number of concentric layers. In this way, immediately after the injection, droplet temperature is radially uniform and every layer has its own fixed temperature equal to fuel injection temperature. As soon as the drop heats up a temperature profile will be established in it, where external layers will be hotter while inner ones will be remain at the fuel injection temperature until they begin to heat up. In this way the droplet temperature profile will be modified during all the vaporisation period. In order to not complicate numerical computations with a very small Δr (which can lead to Δt_{num} time steps of calculations being too small), distances between layers have to be fixed and when the droplet size considerably decreases the number of layers decreases too. A large number of tests have been done to choose the initial number of layers and as a consequence the constant value of Δr, in order to obtain accurate solution but consistent the computational time and capacity. All numerical results shown in this paper use an initial grid of 51 layers inside the droplet.

The diffusion limit model has been coupled with the use of an experimental relation for the tetradecane fuel liquid density [g/cm^3] obtained from Massoli et al., (1993)

$$\rho(T) = \rho(T_0) - 10^{-3}\times 0.69(T-T_0) - 10^{-6}\times 0.13(T-T_0)^2, \tag{6}$$

where T_0 is a reference temperature of 300 K.

In this way introducing the variation of liquid fuel density with temperature, the thermal swelling of the droplet has been taken into account (Belardini et al., 1997).

3. Results and discussion

3.1. Combustion bomb test cases

Before testing the model with a diesel spray, single droplet computations in a combustion bomb (Table 1) were performed to validate the proposed evaporation model.

The proposed evaporation model was tested in a large number of different ambient conditions (air temperature of 473, 573, 673, 950 K and air pressure of 1, 20 and 45 bar). A limited number of droplets of different fuel (Tetradecane, N-heptane, Diesel Fuel) and with different initial diameter (70–280 μm) were injected in the combustion bomb neglecting break-up and coalescence phenomena.

A comparison with numerical computations has been taken from some experimental data presented by Belardini et al. (1992) and obtained by a laser light scattering multi-angle technique. In Fig. 1 the change-over time of the square ratio between the droplet's diameter and its initial value, referring to a tetradecane drop ($R_0 = 36$ μm, $T = 673$ K, $p = 1$ bar), is reported versus time. It can be noticed that, with respect to the Spalding model, the proposed finite conduction model, without considering thermal swelling, overestimates the evaporation rate in the first milliseconds after the injection; while later in the process, it underestimates the vapour mass transfer from the droplet. In the same figure some results obtained from a 'new' model considering simultaneously heat conduction transfer and thermal swelling (Belardini et al., 1997) are presented. This model seems to fit the experimental data better than the Spalding original model during all phases of droplet lifetime.

Considering the internal heat conduction, the faster heating is more evident looking at the diagrams of Fig. 2, where the droplet surface temperature is reported versus time for the

Table 1
Combustion bomb characteristics

Control volume	Comb. Bomb
Dimension	40 mm×20 mm
Injection speed	6 m/s
Injector	1 holes $\phi = 0.28$ mm
Injected mass	10^{-9} g
Injection temperature	300 K
Computer mesh	20×20×40
Reference fuel	Tetradecane

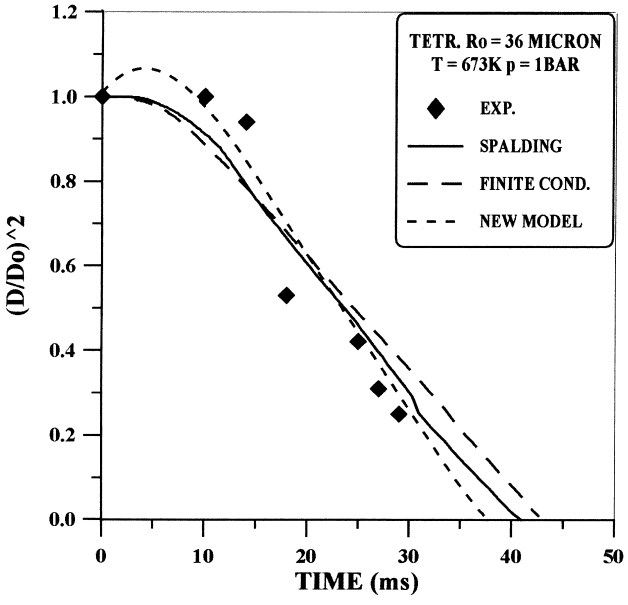

Fig. 1. Droplet diameter versus time.

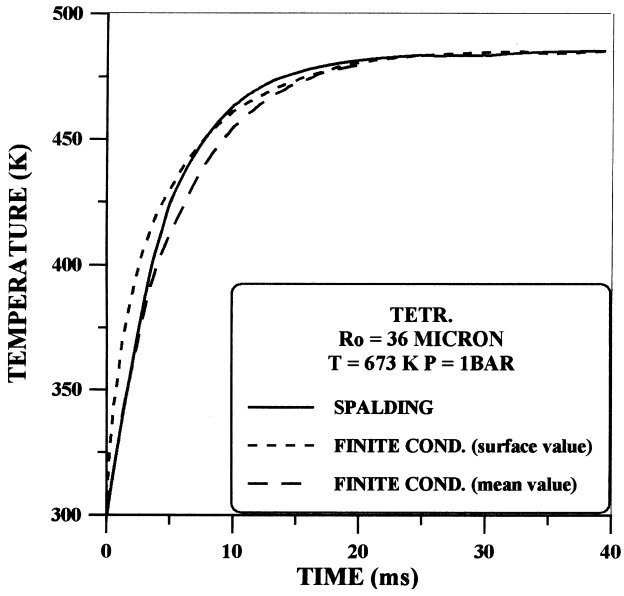

Fig. 2. Droplet temperature versus time.

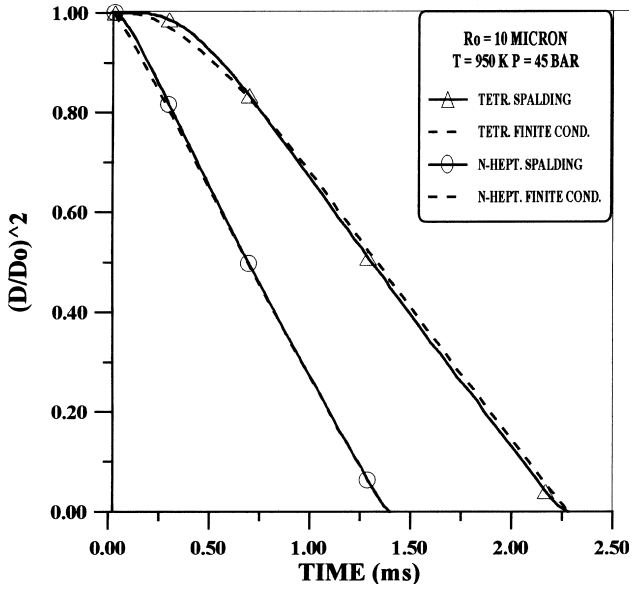

Fig. 4. Comparison between different fuels.

same previous ambient conditions. The modified evaporation model, taking into account the transient heating inside the droplet, gives initially higher droplet surface temperature values while the inner part of the droplet is cool, as demonstrated by the droplet mean temperature curve. It is evident that the trend is reversed in the last part of droplet lifetime when the temperature gradients decrease more quickly than with the original Spalding model. As confirmation, in Fig. 3 the computed temperature distribution inside the droplet at different times from the injection is shown.

In Fig. 4 a comparison between the two models is performed simulating in-cylinder diesel engine environment at the start of the injection process. It is quite evident that differences between both models are less important with a more volatile fuel like N-heptane.

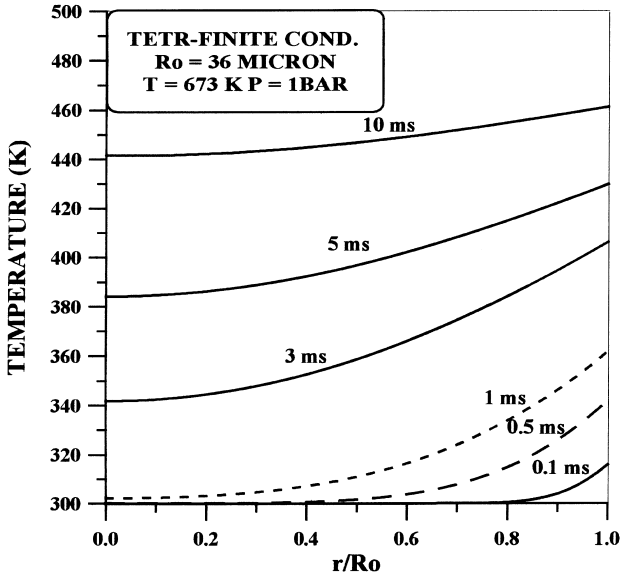

Fig. 3. Temperature distribution within the drop.

3.2. Engine test cases

Numerical test cases have been performed in a combustion chamber of a real single cylinder D.I. diesel engine whose characteristics are reported in Table 2. A grid size of $20\times24\times21$ nodes has been used. The evaporation model used for engine's analysis is the finite conductivity model neglecting thermal swelling; it has been found that the thermal swelling, important for isolated single droplet computations, do not modify significantly numerical results under high temperature and high turbulence conditions present in the combustion chamber of the D.I. diesel engine.

In a diesel engine combustion chamber the very short droplet lifetime is due to the extreme ambient conditions combined with the high injection velocity, high injection pressure, turbulence and atomization effects. The study of the whole fuel spray has required, as a consequence, an adequate modified version of the break-up and coalescence phenomena accounting for internal temperature distribution in droplets. The break-up model is slightly influenced by the evaporation model changes; as a matter of fact break-up rate did not change remarkably even though the surface tension decrease with a higher surface temperature value. Considering an

Table 2
The engine characteristics

Compression ratio	18.0
Bore	100 [mm]
Stroke	95 [mm]
Connecting rod length	178 [mm]
Combustion chamber	Toroidal
Equivalent Aspect Ratio	4.6
Speed	1250 [rpm]
Injector	4 holes $\phi = 0.28$ mm
Angle between two sprays	160
Injection velocity	210 [m/s]
Fuel injected mass	0.02 [g/cycle]
Injection start	7.4 C.A. BTDC
Injection duration	7.0 CA
Fuel	Diesel Fuel

instantaneous molecular mixing after the coalescence between two drops with different temperature distributions, the description of coalescence process was changed in such a way that the new drop had a uniform temperature equal to a mean value.

In order to evaluate the influence of the modified evaporation rate on spray behaviour a preliminary analysis without considering combustion has been done. The spray evolution has been followed by varying the description of the break-up phenomenon and using different break-up models. The most used break-up spray models in CFD computations are based on the analysis of the instability of a liquid column injected unbroken from the nozzle orifice (WAVE model), or on the analogy between a damped spring mass system and a liquid droplet (TAB Model). These break-up models have been used here with a set of constants chosen by Beatrice et al., 1995. Considering that the TAB model underestimates the tip penetration while the WAVE model overestimates it, the 'hybrid' model has been tested as follows: at the beginning of the injection process the WAVE model is used, allowing for the high diameter of the injected liquid droplets. After that, when the droplet diameter becomes less than 95% of the maximum diameter of the injected drops the TAB model is used. The choice to use both models has a physical meaning; in fact, for large diameters drops, as expected near the nozzle exit, the model of unstable wave propagation on a liquid surface may be more relevant. Later during the injection process, the compution of break-up with the TAB analogy seems to be more appropriate for the smaller drops.

Numerical results in terms of typical spray characteristics are presented in Fig. 5 spray tip penetration, Sauter mean Diameter versus distance from the nozzle and vapour mass quantities. In Fig. 5a the spray tip penetration is reported versus crank angle, comparing the results obtained with the proposed evaporation model and the original Spalding model, for the two different atomization models mentioned above. Some experimental data, obtained from an in-cylinder high speed cinematography technique (Beatrice et al., 1995), have

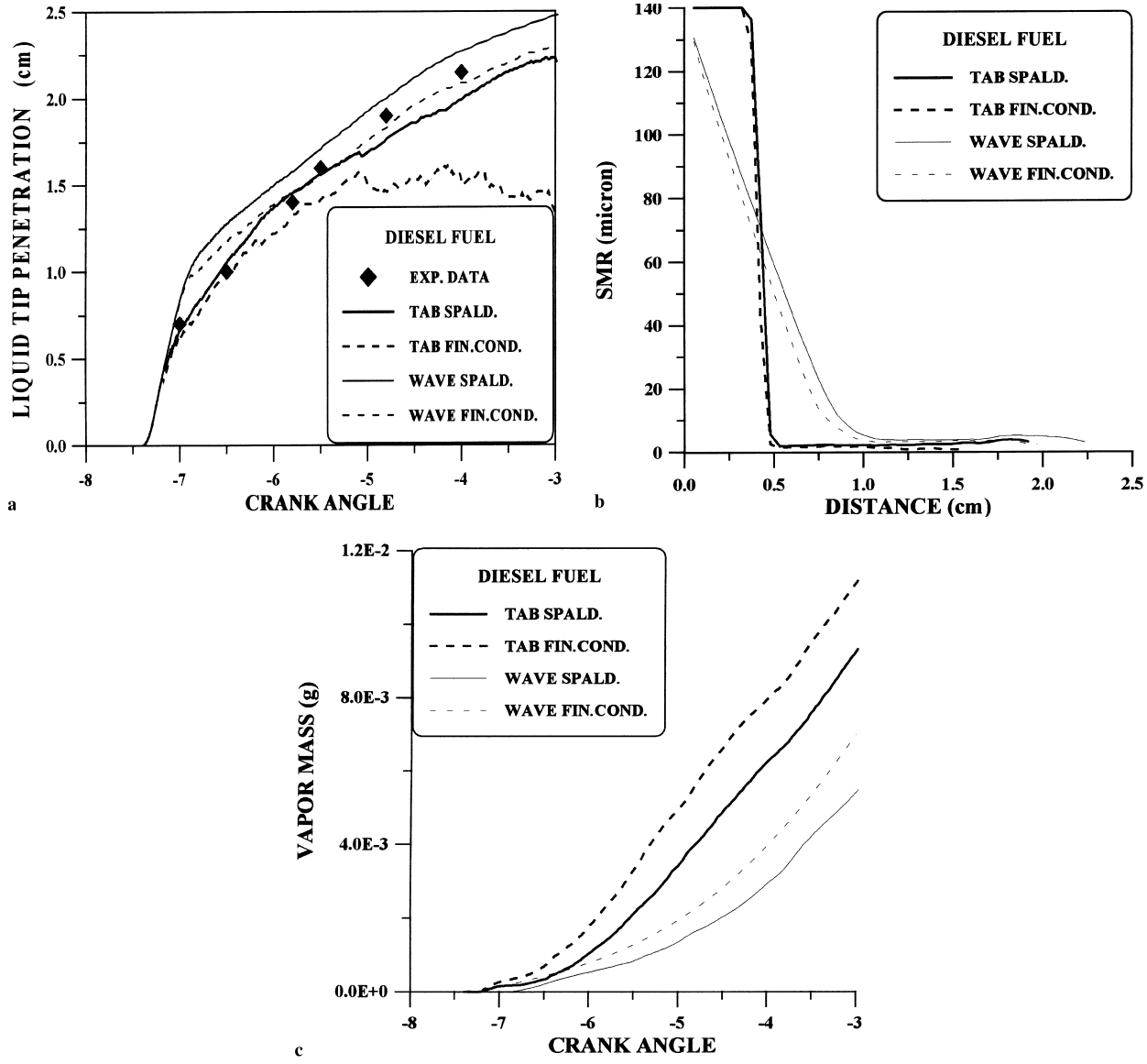

Fig. 5. Tip penetrations (a), SMR (b) and Vapour mass (c) obtained with Spalding and Finite Conductivity evaporation models varying the break-up model.

been used as a reference for the numerical data. It can be noticed how the penetration obtained with the modified evaporation model is lower with both break-up models. On the other hand, the droplet size distribution, in terms of SMR (Fig. 5b), considering an initial SMR value of 140 μm, with the modified evaporation model is lower with respect to the one obtained with the original evaporation model. The evaporation rate for the finite conductivity evaporation model is higher accounting for higher values of the surface droplet temperature during its transient heating; in Fig. 5c the vapour mass quantities in the combustion chamber are shown. The influence of the evaporation effects are more important in the case of the TAB model then the WAVE model, due to the different droplet size distribution. As a matter of fact, as evident in Fig. 5b, the slope of SMR is very much different with TAB model because of its tendency to break the droplets quickly (Beatrice et al., 1995). For a deeper investigation of the phenomenon it can be useful to analyze the fuel/air density ratio distributions in the spray zone. In Figs. 6, 7, 8 and 9 the cross and meridional sections at 3 c.a. BTDC of the distributions with both break-up models are shown, comparing the two evaporation model effects. The pictures confirm the tendency of the new evaporation model to create more vapour, showing also a larger vapour zone on the jet tip. This effect is more evident when using TAB model, because of its tendency to produce smaller droplets.

In Fig. 10a the curves of spray tip penetration for both evaporation models are reported in the case of the 'hybrid' break-up model. Even in this case the modified evaporation model brings a lower tip penetration with a higher vapor mass quantity. The increased evaporation rate is also evident from the Fig. 10b, where the sauter mean radius are reported for conditions as previously reported.

To analyze the influence of the modified evaporation model on combustion evolution and exhaust emissions, a further number of numerical test cases have been performed in the same single cylinder Direct Injection (DI) diesel engine (Table 3) by injecting tetradecane fuel. All numerical runs were tested with the TAB atomization model. The injection apparatus comprises a Bosch P-type in line pump and a four hole injector, with a cone angle between the sprays of 160°. The injection pump was fitted on an in-house machined device allowing variation of the injection timing during the engine running. With a proper choice of plunger diameter and of injection pipe bore to length ratio, a very stable operation at low-test speed allows control of the cyclic variation of the injection below 1%. The engine head was equipped with two optical accesses used for two colour measurements and high speed cinematography, and with a second head, in which a fast acting valve allows the direct sampling of the combustion products. The fast valve is located in the combustion chamber at about the same radial position of one of the optical access points allowing one to relate the soot optical measurements and the sampled species measurements. The electronic control system of the valve is able to open the needle for about 5–7 C.A. degrees at 1250 rpm engine speed for each engine combustion cycle. This window

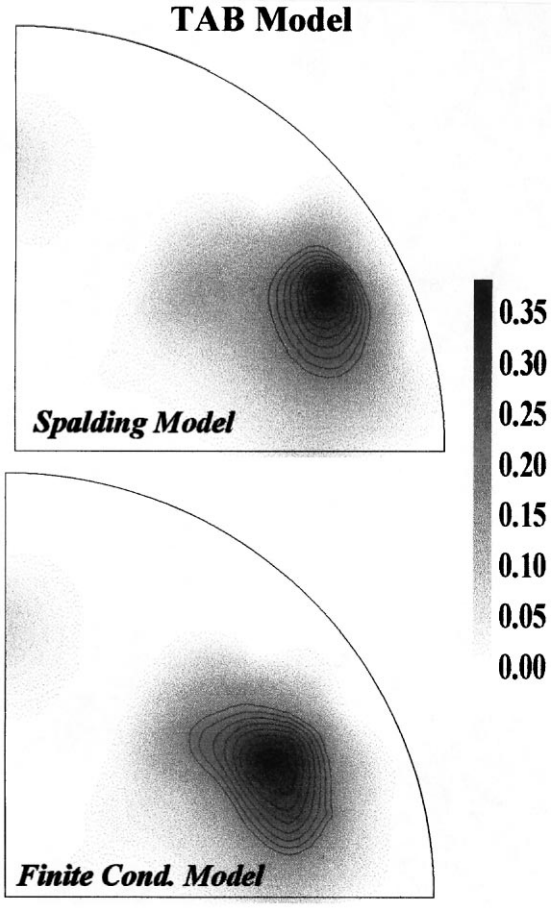

Fig. 6. Cross section of the local fuel/air ratio distributions (plane $k = 8$).

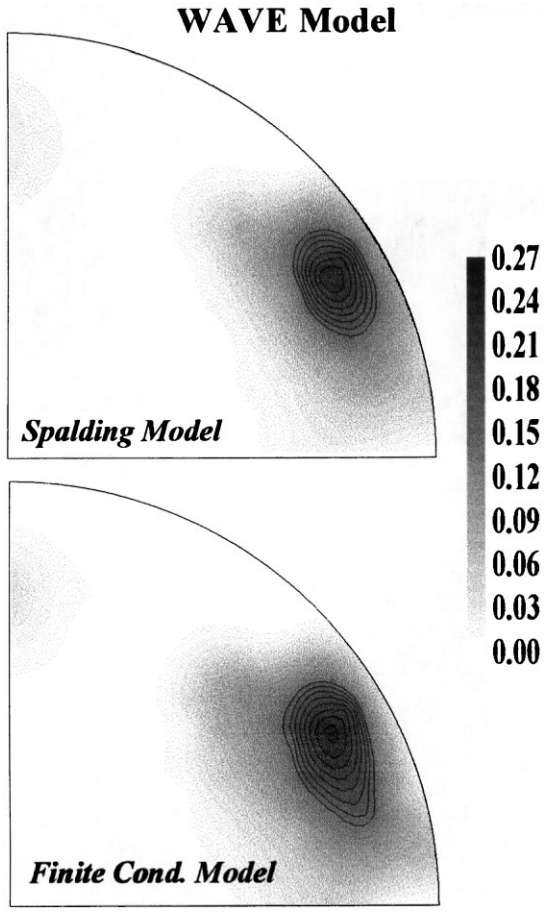

Fig. 7. Cross section of local fuel/air ratio distributions (plane $k = 8$).

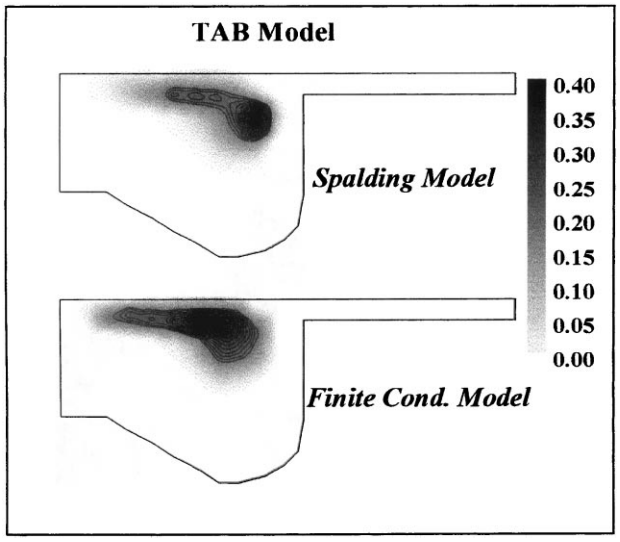

Fig. 8. TAB model: meridional section of local fuel/air ratio distributions (plane $j=4$).

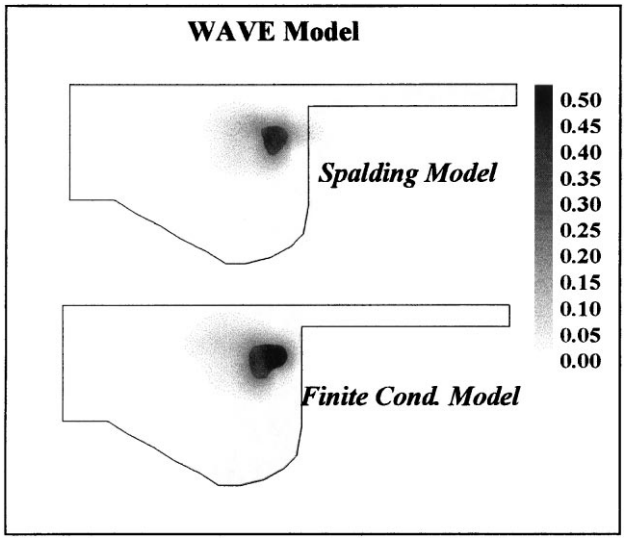

Fig. 9. Wave model: meridional section of fuel/air ratio distributions (plane $j=4$).

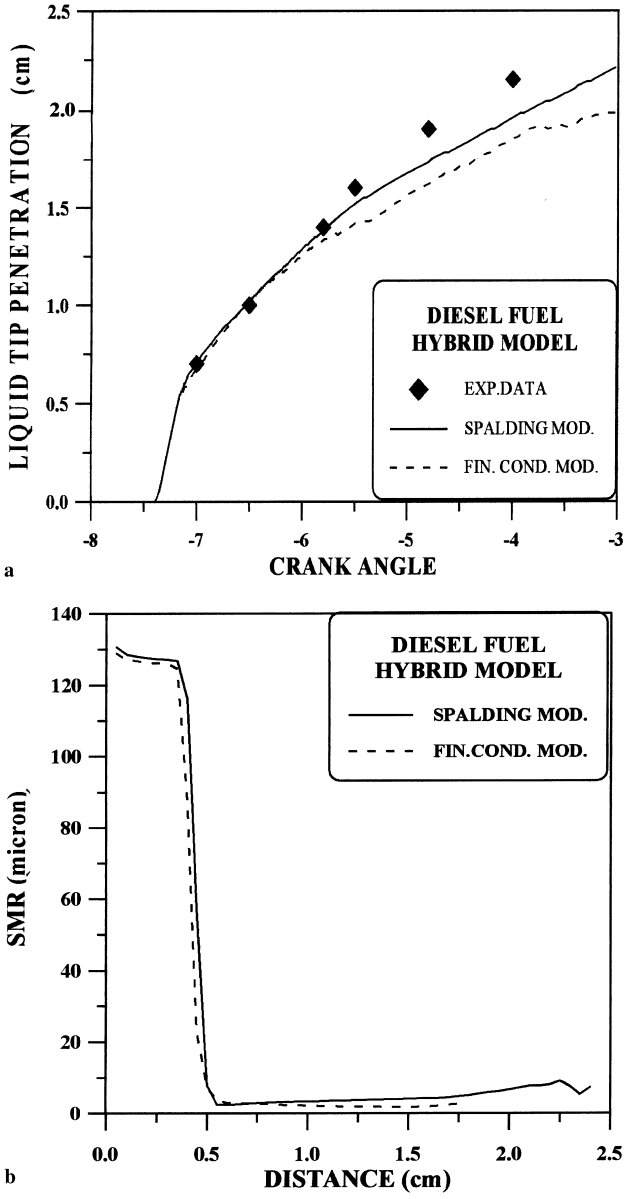

Fig. 10. (a) Liquid Tip penetration obtained with Spalding and Finite Conductivity evaporation models using the 'hybrid' break-up model. (b) SMR obtained with Spalding and Finite Conductivity evaporation models using the 'hybrid' break-up model.

can be shifted to different timings with a suitable control unit allowing, by an ensemble average technique, to obtain the concentration profile of the different combustion products during the engine cycle. The sampling procedure was repeated for as many as 100,000 combustion cycles to collect a significant amount of gaseous species products.

In Fig. 11 tetradecane liquid spray distributions in the combustion chamber are shown until the start of combustion for the Spalding evaporation model and the proposed model. As further confirmation of the previous statements, it can be observed that the new evaporation model influences spray tip penetration and liquid mass quantities. It is quite evident that the new model's effects on tetradecane combustion are also relevant. In Fig. 12 computational results are reported in terms of in-cylinder pressure. The higher vapour mass quantity present in the combustion chamber after the ignition delay time brings a faster combustion rate in the premixed combustion evolution, and as a consequence, to a higher pressure peak value. This fact can be further explained by the diagrams of Fig. 13, where the burned fuel mass is reported Vs crank angle; the burned fuel mass obtained from the finite conductivity model reaches higher values than the Spalding model. Some others tests have referred to a more volatile fuel like N-heptane. In this case the differences between the evaporation models are less important because the droplet lifetime is extremely short.

To analyze the influence of the evaporation model formulation on in cylinder species predictions, numerical and measured combustion species were sampled in a control volume in the combustion chamber, located at 4 mm below the engine head, downstream one of the four fuel jets, at about 15° with respect to the jet axis and at 20 mm from the nozzle outlet. It must be noted that these results are the picture of a small

Table 3
Diesel engine characteristics

Engine	D.I. Diesel
Compression ratio	18.0
Bore	10.0 [cm]
Stroke	9.5 [cm]
Connecting rod length	17.8 [cm]
Combustion chamber	Toroidal
Speed	1250 [rpm]
Injector	4 holes $\phi = 0.28$ mm
Injection speed	140 m/s
Injected mass	0.02 g/cycle
Reference fuel	Tetradecane
Injection timing	3.6 B.T.D.C
Injection duration	7.0 CA
Computational Mesh	$20 \times 20 \times 21$

volume inside the combustion chamber. This is an important remark, because in our opinion a 3D code should be able to keep the details of the combustion process. The molecular oxygen evolution in fast sampling control volume is shown in Fig. 14 in comparison with the experimental data (Belardini et al., 1996a,b). Due to the faster vaporisation produced by the finite conductivity model, the oxygen consumption in the control volume is slightly higher (+2.5%) in the diffusive phase of combustion with respect the standard Spalding model. The computed NO_x concentration is compared with the experimental one (Belardini et al., 1996a,b) in the diagrams of the

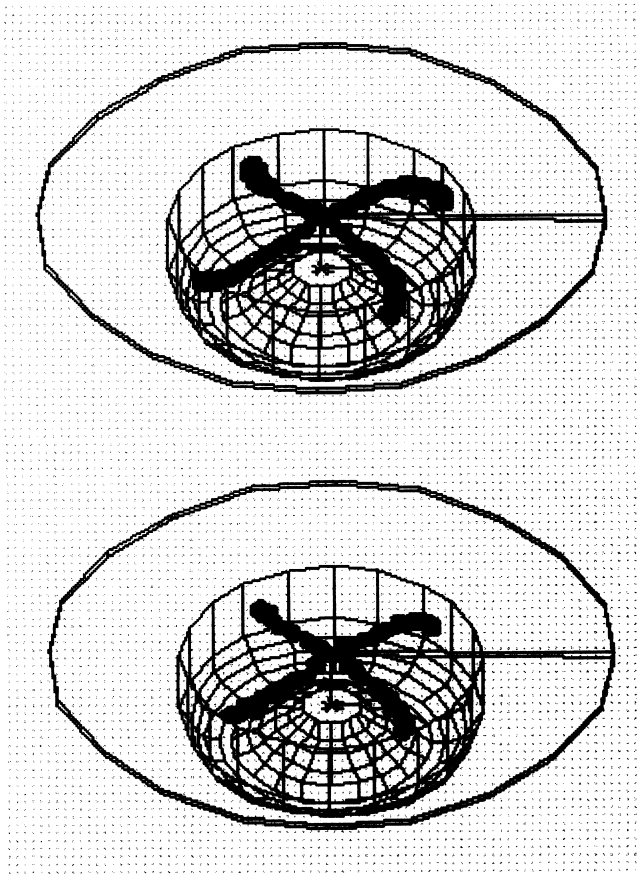

Fig. 11. Liquid Spray distribution for the Spalding (top) and Finite Conduction Model (bottom).

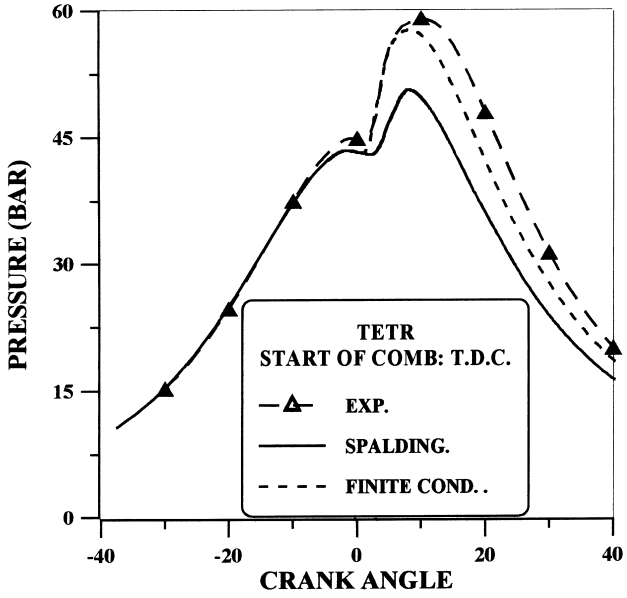

Fig. 12. In-cylinder pressure versus crank angle.

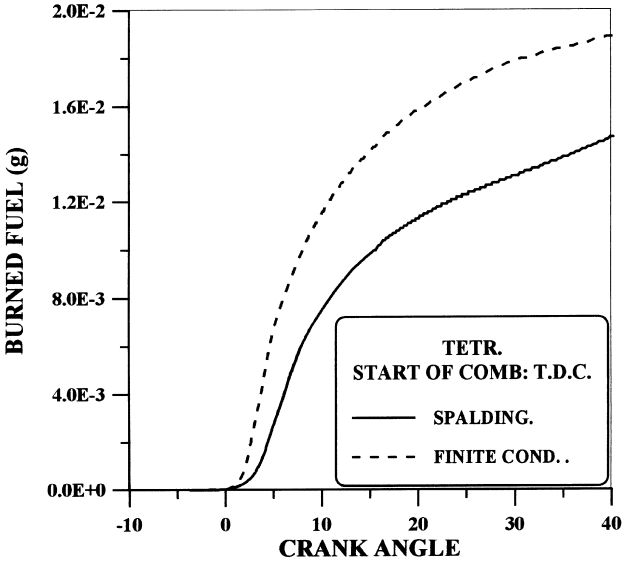

Fig. 13. Burned fuel versus crank angle.

Fig. 15. Because of the higher temperature values in the combustion chamber and the more complete fuel mass consumption exhibited by the new model, the predicted NO_x concentration fits very well the experimental data. However these are only preliminary results and more detailed studies are needed because much attention must be spent to properly evaluate the measurement volume; when the control volume is positioned differently, the comparison between numerical and experimental data gives different results. This is an additional problem in accuracy that must be carefully evaluated.

4. Conclusions

In the present work the performances of an improved version of the vaporisation model, implemented in the Kiva II

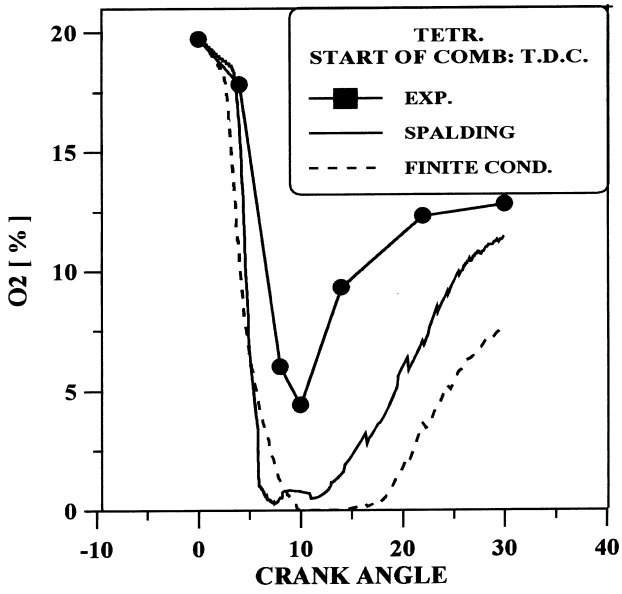

Fig. 14. Oxygen consumption versus crank angle.

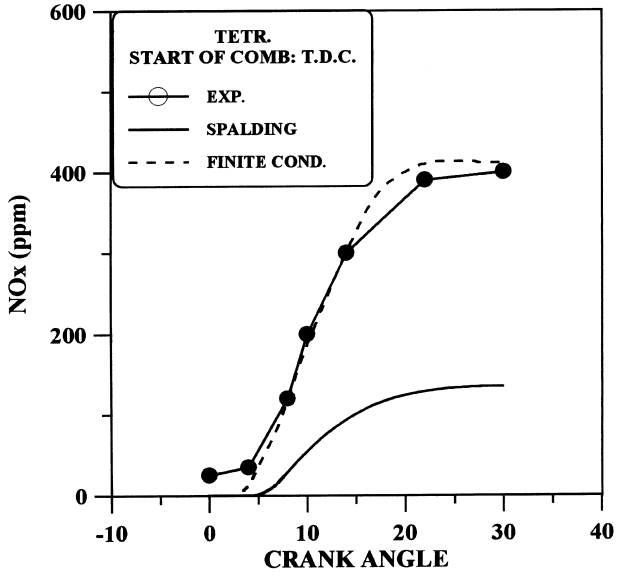

Fig. 15. NO_x production versus crank angle.

code was investigated. In particular the introduction of a temperature distribution inside the droplets was evaluated. To this end, the phenomenon was first studied in a combustion bomb simulating single droplet experiments and in a second phase in an actual diesel engine simulating the whole spray and combustion behaviour. In agreement with the results in the combustion bomb, the finite conductivity model bring a more appropriate evaporation rate. A preliminary analysis on the effect of the new model on in-cylinder combustion species was also carried out. Due to some uncertainties in comparing measured and computed species concentration, more detailed studies are needed in order to evaluate the consequence of the finite conduction model on pollutants predictions.

References

Abramzon, B., Sirignano, W.A., 1988. Droplet Vaporisation model or spray combustion calculations. AIAA 26th Aerospace Sciences meeting.

Aggarwal, S.K, 1987. Modeling of a dilute vaporizing multicomponent fuel spray. Internat. J. Heat Mass Transfer 30, 1949–1961.

Amato, U., Belardini, P., Bertoli, C., DelGiacomo, N., 1991. The joint use of multidimensional modeling and field experiments in order to design diesel combustion systems. IMEchE : London, pp. 430–445.

Amsden, A.A., O'Rourke, P.J., Butler, T.D., 1989. KIVA-II: A computer program for chemically reactive flows with sprays. Los Alamos National Laboratory Report No. LA-11560-MS.

Arcoumanis, C., Gavaises, M., French, B., 1997. Effect of fuel injection processes on the structure of diesel sprays. SAE Paper 970799.

Beatrice, C., Belardini, P., Bertoli, C., Cameretti, M.C., Cirillo, N.C., 1995. Fuel jet models for multidimensional diesel combustion calculation: an update. SAE Paper 950086.

Belardini, P., Bertoli, C., Lazzaro, M., Massoli, P., 1992. Single droplet evaporation rate: experimental and numerical investigations. In: Proceedings of the Second International Conference on Fluid-mechanics, Combustion, Emissions and Reliability in Reciprocating Engines, Capri, Italy, pp. 265–270.

Belardini, P., Bertoli, B.C., Del Giacomo N., Cameretti M.C., 1996. A simple autoignition model for 3D diesel combustion computations. IMechE Transactions, 1, C499/047, London, pp. 305–315.

Belardini, P., Bertoli, B.C., D'Anna, A., Del Giacomo, N., 1996. Application of a reduced kinetic model of soot formation and burnout in 3D diesel combustion computations. XXVI Symposium on Combustion.

Belardini, P., Bertoli, C., Cameretti, M.C., Migliaccio M.na, 1997. Influence of evaporation model formulations on spray behaviour in 3D computations of diesel combustion. Atti del Conference on Liquid Atomization and Spray systems ILASS, Firenze.

Bowman, C.T., 1975. Kinetics of pollutant formation and decsription in combustion. Prog. Energy Combust. Sci. 1, 33–45.

Golini, S., 1993. Combustione: motori diesel e ad accensione comandata, Tesi di dottorato di ricerca in Energetica, Università La Sapienza.

Hardenberg, H.O., Hase, F.W., 1979. An empirical formula for computing pressure rise delay of a fuel from its cetane number and from relevant parameters of D.I. diesel engines. SAE Paper 790493.

Hiroyasu, H., Kadota, T., Arai, M., 1980. Supplementary comments: fuel spray characteristics in diesel engines. In: Combustion Modeling in Reciprocating Engines. Plenum Press, New York, pp. 369–405.

Kneer, R., Hohmann, S., Klingsporn, Renz, U., 1996. An improved model to describe spray evaporation under diesel-like conditions. SAE Paper 960630.

Hohmann, S., Klingsporn, Renz, U., 1996. An improved model to describe spray evoporation under diesel-like conditions. SAE Paper 960630.

Jin, J.D., Borman G.L., 1985. A model for multicomponent droplet vaporisation at high ambient pressures. SAE Paper 850264.

Maxwell, J.B., 1977. Data Book on Hydrocarbons. Krigier Publishing Company, Huntington, New York.

Massoli, P., Beretta, F., D'Alessio, A., Lazzaro, M., 1993. Temperature and size of single transparent droplets by light scattering in the forward and rainbow regions. Appl. Optics, vol. 32, No. 18.

Naber, J.D., Enright, B., Farrel, P., 1988. Fuel impingement in a direct injection diesel engine. SAE Paper 881316.

Nishida, K., Hiroyasu, H., 1989. Simplified 3D modelling of mixture formation and combustion in a D.I. diesel engine. SAE paper 890269.

O'Rourke, P.J., Amsden, A.A., 1987. The TAB method for numerical calculation of spray droplet breakup. SAE Paper 872089.

Patterson, M.A., Reitz, R.D.Abramzon, B., Sirignano, W.A., 1988. Modeling the effects of fuel spray characteristics on diesel engine combustion and emision. SAE Paper 980131.

Reitz, R.D., 1987. Modeling atomization processes in highpressure vaporising sprays. Atomization and Sprays 3, 309–337.

Shwing-ChungWong, Ar-Cheng, L., 1992. Internal temperature distributions of droplets vaporizing in high-pressure convective flows. J. Fluid Mech. 237, 671–687.

Sirignano, W.A., 1978. Theory of multi-component fuel droplet vaporisation. Arch. Thermodynamics Combustion 9 (2), 231–247.

Spalding, D.B., 1953. The combustion of liquid fuels. In: Proceedings of the Fourth International Symposium on Combustion, The Combustion Institute, Pittsburgh, PA.

Tennison, P.,J., Georjon, T.L., Farrel, P.V., Reitz, R.D., 1998. An experimental and numerical study of sprays from a common rail injection system for use in an HSDI diesel engine. SAE Paper 980810.

Varnavas, C., Assanins, D.N., 1996. A high temperature and high pressure evaporation model for the KIVA-3 code. SAE Paper 960629.